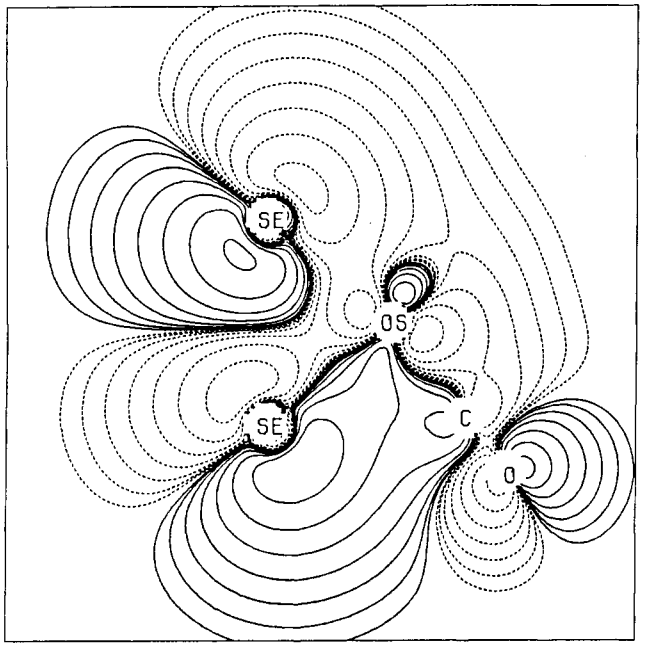


**Figure 5.** Orbital plot of 6a′ in the *yz* (mirror) plane. The lowest contour values are $2.44 \times 10^{-4}$ e au$^{-3}$, and each succeeding contour differs from the previous one by a factor of 2.0.

on S and has substantial lone-pair character. We believe that 6a′ plays an important role in these condensation reactions. For example, in the insertion of a $PtL_2$ fragment into an Os*–S bond, the crystal structure of the insertion product[4d] shows the $PtL_2$ fragment opposite the unique carbonyl on Os* (Pt–Os*–C ≃ 166°). This stereochemistry would be consistent with electrophilic attack on the Os*–S bond opposite the unique carbonyl. Our calculations show that the amount of S character in the 6a′ orbital is twice as large for the S opposite the unique carbonyl (the upper chalcogen in Figure 5) as it is for the other S (43% vs 21%). Thus, the upper S has the more available chalcogen electrons. This is also reflected in the relative numbers of contours in Figure 5.

To date, only $Os(CO)_4$ has been inserted into an osmium–chalcogen bond in $Os_3(CO)_9Se_2$.[29] Because of very similar electronic structures and with even more available chalcogen electron density (6a′ is destabilized by 0.56 eV) than in the S homologue, $Os_3(CO)_9Se_2$ should develop a condensation chemistry comparable to that of $Os_3(CO)_9S_2$.

(29) Adams, R. D.; Horvath, I. T. *Inorg. Chem.* **1984**, *23*, 4718.

### Conclusion

Through the study of Os homologues of $Fe_3(CO)_9S_2$ we have clarified the bonding and spectral assignments of these clusters. The HOMO is a M–M–M 3c-2e bond that contains most of the metal–metal bonding population. Nearly all of the net cluster bonding uses the $e_g$- and $a_1$-like fragment orbitals. The $t_{2g}$-like fragment orbitals mix heavily into the cluster bonding and antibonding orbitals but result in little net contribution to metal–metal or metal–chalcogen bonds. The metal–chalcogen interactions are much stronger than the metal–metal interactions, as demonstrated in the relative gaps between orbitals 7a″, 10a′, and 8a″.

In $Fe_3(CO)_9S_2$ all of the orbitals with substantial sulfur character were beneath the molecular orbitals derived solely from the $t_{2g}$-like sets. In the osmium homologues there was an orbital (6a′) with substantial chalcogen character in the midst of the $t_{2g}$-derived orbitals. The calculations show that 6a′ is destabilized by 0.56 eV when S is replaced by Se. This shift from band D to band C can be seen in the spectra of $Os_3(CO)_9X_2$, X = S and Se, respectively. We believe that 6a′ has substantial chalcogen lone-pair character, which we propose is important in the nucleophilic attack of this cluster on metal–ligand groups containing low-lying unoccupied orbitals.

We are unable to reconcile resonance structures **1** and **2** with the observed structures of the osmium clusters. All metal–metal and metal–chalcogen bonds appear to be full single bonds. A possible solution of this dilemma would be the addition of an electron pair beyond the seven pairs required by SEP theory. A potential source of this extra electron pair may be one of the fragment $t_{2g}$-like orbitals. The only alternative would be to assume that the Os–Os bond lengths are insensitive to the Os–Os bond order and that the calculations, which favor resonance structure **1**, are essentially correct.

**Acknowledgment.** We thank the Robert A. Welch Foundation (Grant No. A-648) for the support of this work and the National Science Foundation for funds to purchase the VAX 11/780.

**Registry No.** $Os_3(CO)_9(\mu_3\text{-}S)_2$, 72282-40-7; $Os_3(CO)_9(\mu_3\text{-}Se)_2$, 72282-41-8.

Contribution from the Department of Chemistry, Colorado State University, Fort Collins, Colorado 80523, and Los Alamos National Laboratory, Los Alamos, New Mexico 87545

# Electronic and Molecular Structure of $OTeF_5^-$

P. K. Miller,[1a] K. D. Abney,[1b] A. K. Rappé,[1a] O. P. Anderson,[1a] and S. H. Strauss*,[1a,2]

*Received November 3, 1987*

Salts of the $OTeF_5^-$ anion were investigated by IR and Raman spectroscopy and by X-ray crystallography. Experimental results were compared with ab initio Hartree–Fock calculations on the $OTeF_5$ radical, $Na^+OTeF_5^-$, and the singlet and triplet states of the free $OTeF_5^-$ anion. The compound $[(PS)H^+][OTeF_5^-]$ was examined by single-crystal X-ray crystallography ($(PS)H^+$ = protonated 1,8-bis(dimethylamino)naphthalene): $P\bar{1}$, $a$ = 8.241 (1) Å, $b$ = 8.768 (2) Å, $c$ = 12.591 (3) Å, $\alpha$ = 74.08 (2)°, $\beta$ = 78.00 (2)°, $\gamma$ = 80.23 (2)°, $Z$ = 2, $T$ = −106 °C. Unlike other salts of the $OTeF_5^-$ anion, $[(PS)H^+][OTeF_5^-]$ did not exhibit any O/F disorder. Since the spectroscopic data for $[(PS)H^+][OTeF_5^-]$ closely matched those of $[N(n\text{-}Bu)_4^+][OTeF_5^-]$, it was concluded that this structure contains the best approximation of the structure of the free $OTeF_5^-$ anion. The librationally corrected results are Te–O = 1.803 Å, Te–$F_{ax}$ = 1.872 Å, Te–$F_{eq}$ = 1.870 Å (average), and O–Te–$F_{eq}$ = 95.2° (average). A normal-coordinate analysis of $OTeF_5^-$ was carried out by using this geometry and spectroscopic data for the $^{16}O$ and $^{18}O$ equivalents of $[N(n\text{-}Bu)_4^+][OTeF_5^-]$.

### Introduction

Studies of metal and non-metal $OTeF_5$ (teflate) compounds have been aided by the spectroscopic and structural probes afforded by the $OTeF_5$ group: the Te–O distance, the TeO stretching frequency ($\nu$(TeO)), and the $^{19}F$ NMR chemical shift of the fluorine atom trans to oxygen.[3-8] These parameters vary

(1) (a) Colorado State University. (b) Los Alamos National Laboratory.
(2) Alfred P. Sloan Fellow, 1987–1989.

(3) Strauss, S. H.; Abney, K. D.; Anderson, O. P. *Inorg. Chem.* **1986**, *25*, 2806.

0020-1669/88/1327-2255$01.50/0 

in a characteristic and understandable way depending on the nature of the element to which the teflate oxygen atom is bonded or ion paired as well as the strength of that interaction. The extremes of covalent and ionic bonding of teflate groups can be represented by $F_5TeO$–$OTeF_5$[9] and the $OTeF_5^-$ anion, respectively.

Reasonable models for free, ionic $OTeF_5^-$ are salts such as $Cs^+OTeF_5^-$[10] and $[N(n\text{-}Bu)_4^+][OTeF_5^-]$,[3] which exhibit the highest $\nu$(TeO) values for known teflate compounds, 873 and 867 $cm^{-1}$, respectively. However, because of the similarities in covalent and van der Waals radii of oxygen and fluorine atoms, these salts are not suitable for detailed structural analysis. X-ray powder photographic results[11] show that $Cs^+OTeF_5^-$ adopts the rhombohedral $KOsF_6$ structure;[12,13] the unit cell parameters for $Cs^+OTeF_5^-$[11] and $Cs^+SbF_6^-$[12] are the same to within experimental error. The crystal symmetry of $Cs^+OTeF_5^-$ requires a minimum 3-fold oxygen/fluorine disorder, and there is every reason to expect that the situation would be at least as unfavorable for $[N(n\text{-}Bu)_4^+][OTeF_5^-]$.

In this paper we report the synthesis and spectroscopic characterization of $H^{18}OTeF_5$ and several salts of $OTeF_5^-$ and $^{18}OTeF_5^-$. The structure of the compound $[(PS)H^+][OTeF_5^-]$ is presented ($(PS)H^+$ is the protonated form of 1,8-bis(dimethylamino)naphthalene (Proton Sponge)). In this compound, the oxygen and fluorine atoms are not disordered. Furthermore, the Te–O and Te–F stretching frequencies of this salt are nearly identical with those of $[N(n\text{-}Bu)_4^+][OTeF_5^-]$. Using structural results from the $(PS)H^+$ salt as well as isotopic data from IR and Raman spectra, we present an improved vibrational analysis of the free teflate anion. Ab initio Hartree-Fock calculations for the $OTeF_5$ radical, $Na^+OTeF_5^-$, and the singlet and triplet states of $OTeF_5^-$ are also presented and compared with the Hartree–Fock results for $TeF_6$.[14]

## Experimental Section

**General Procedures.** In the following preparations and physical measurements, all operations were carried out with rigorous exclusion of dioxygen and water.[15]

**Reagents and Solvents.** Reagents and solvents were reagent grade or better and were dried by standard techniques.[15] The compound 1,8-bis(dimethylamino)naphthalene ($C_{14}H_{18}N_2$), sold by Aldrich under the trade name Proton Sponge, was purified by vacuum sublimation. Calcium hydride ($CaH_2$, Alfa), $TeF_6$ (Ozark-Mahoning), $H_2{}^{18}O$ (Cambridge Isotope), and concentrated sulfuric acid (Fisher) were used as received. The compounds $HOTeF_5$,[3,16,17] $[N(n\text{-}Bu)_4^+][OTeF_5^-]$,[3] $[NEt_3H^+][OTeF_5^-]$,[3] and $Cs^+OTeF_5^-$,[10] were prepared by literature procedures. The salt $[N(n\text{-}Bu)_4^+][^{18}OTeF_5^-]$ was prepared by using the procedure for $[N(n\text{-}Bu)_4^+][OTeF_5^-]$ with $H^{18}OTeF_5$ (see below) in place of $HOTeF_5$.

**Physical Measurements. NMR Spectroscopy.** Samples for $^{19}F$ and $^1H$ NMR spectroscopy were dichloromethane or dichloromethane-$d_2$ solutions with 1% $CFCl_3$ and/or 1% $Me_4Si$ added. Chemical shifts ($\delta$ scale) are relative to these internal standards. All spectra were recorded on a Bruker SY-200 spectrometer at the indicated frequencies: $^{19}F$, 188.31 MHz; $^1H$, 200.13 MHz. All $^{19}F$ NMR spectra were $AB_4X$ patterns upfield of $CFCl_3$ (X = $^{125}Te$, 7.0% natural abundance, $I = {}^1/_2$).

**Vibrational Spectroscopy.** Samples for IR spectroscopy were mulls (Nujol, KBr or polyethylene windows) or dichloromethane solutions (0.2-mm path length ZnS cells). Room-temperature spectra were recorded on either a Perkin-Elmer 983 or a Nicolet 60 SX spectrometer calibrated with polystyrene. For all IR spectra peak positions are ±1 $cm^{-1}$. Samples for Raman spectroscopy were crystalline or polycrystalline solids loaded into glass capillaries. Spectra were recorded with either a Spex Ramalog 5 spectrometer (514.5-nm excitation) or a Spex 1403 spectrometer (514.5-nm excitation). Band positions for Raman spectra are also ±1 $cm^{-1}$.

**Table I.** Experimental Parameters for the X-ray Diffraction Study of $[(PS)H^+][OTeF_5^-]$ ($(PS)H^+ = C_{14}H_{19}N_2^+$)

| | |
|---|---|
| fw | 453.9 |
| space group | $P\bar{1}$ |
| unit cell dimens | |
| $a$, Å | 8.241 (1) |
| $b$, Å | 8.768 (2) |
| $c$, Å | 12.591 (3) |
| $\alpha$, deg | 74.08 (2) |
| $\beta$, deg | 78.00 (2) |
| $\gamma$, deg | 80.23 (2) |
| unit cell vol, Å$^3$ | 849.6 (3) |
| $Z$ | 2 |
| $d$(calcd), g $cm^{-3}$ | 1.77 |
| cryst dimens, mm | 0.12 × 0.26 × 0.50 |
| data collcn temp, °C | −106 (1) |
| radiation (λ, Å) | Mo K$\alpha$ (0.710 73) |
| monochromator | graphite |
| abs coeff, $cm^{-1}$ | 18.8 |
| $2\theta$ range, deg | 4–50 |
| reflcns | $\pm h,k,\pm l$ |
| no. of reflcns | 2768 ($\|F\| > 2.5\sigma(F)$) |
| total no. of reflcns measd | 3323 |
| scan type | $\theta$–$2\theta$ |
| scan speed, deg $min^{-1}$ | variable (2–30) |
| data/param ratio | 12.4 |
| $R$ | 0.0249 |
| $R_w$ | 0.0391 |
| GOF | 2.48 |
| $g$(refined) | $1.6 \times 10^{-4}$ |
| slope of normal probability plot | 1.85 |

**Preparation of Compounds. $[pyH^+][OTeF_5^-]$ and $[lutH^+][OTeF_5^-]$.** Equivalent amounts of $HOTeF_5$ and either pyridine (py) or lutidine (lut) were mixed in dichloromethane. Cooling the solution below 0 °C resulted in crystallization of the salts in better than 80% yield. $^{19}F$ NMR ($CD_2Cl_2$): for $[pyH^+][OTeF_5^-]$, $\delta_A$ −26.9, $\delta_B$ −41.6, $J_{AB}$ = 176 Hz, $J_{AX}$ = 2910 Hz, $J_{BX}$ = 3560 Hz; for $[lutH^+][OTeF_5^-]$, $\delta_A$ −25.5, $\delta_B$ −40.2, $J_{AB}$ = 175 Hz, $J_{AX}$ = 2869 Hz, $J_{BX}$ = 3576 Hz.

**$[(PS)H^+][OTeF_5^-]$.** Equivalent amounts of Proton Sponge (PS) and $HOTeF_5$ were mixed in dichloromethane. Slow evaporation of the solution at 22 °C resulted in crystallization of the salt in ca. 90% yield. $^{19}F$ NMR ($CD_2Cl_2$): $\delta_A$ − 20.0, $\delta_B$ −37.4, $J_{AB}$ = 170 Hz, $J_{AX}$ = 2689 Hz, $J_{BX}$ = 3643 Hz. $^1H$ NMR ($CD_2Cl_2$): $\delta$ 19.0 (1 H, br s), 8.0 (2 H, dd, $J$ = 8.1, 1.1 Hz), 7.8 (2 H, dd, $J$ = 7.6, 1.1 Hz), 7.7 (2 H, dd, $J$ = 8.1, 7.6 Hz), 3.2 (12 H, d, $J$ = 2.7 Hz). The oxygen-18 salt was prepared in a similar fashion by using $H^{18}OTeF_5$ (see below) in place of $HOTeF_5$.

**$H^{18}OTeF_5$.** The compound $Ca(^{18}OH)_2$ was generated in situ by adding $H_2{}^{18}O$ (1.0 mL, 56 mmol) to a slurry of $CaH_2$ (1.17 g, 28 mmol) and pyridine (40 mL). Hydrogen gas was vented through a mineral oil bubbler. The reaction mixture was stirred and sonicated for 3 days at room temperature to ensure complete reaction, after which it was degassed by freeze–pump–thaw cycles. Tellurium hexafluoride (13.5 g, 56 mmol) was added to the frozen (−196 °C) reaction mixture by vacuum transfer, after which the mixture was heated to 45 °C and stirred for 12 h. *Caution!* The pressure inside the reaction flask can exceed 1 atm depending on the amount of $TeF_6$ (bp −38 °C) used and the size of the flask; the $TeF_6$ may be added in smaller aliquots, with 6 h of heating and stirring between aliquots.

Pyridine and any unreacted $TeF_6$ were removed under vacuum, leaving a white solid mixture of $CaF_2$ and $[pyH^+][^{18}OTeF_5^-]$. The latter salt was extracted into warm dichloromethane by using a continuous extraction filter frit. Removal of dichloromethane under vacuum left a white residue of $[pyH^+][^{18}OTeF_5^-]$, which has a $^{19}F$ NMR spectrum identical with that of the natural abundance compound (see above). The oxygen-18 pyridinium salt was treated with a large excess of concentrated sulfuric acid. Vacuum distillation of the $H^{18}OTeF_5$ that was formed through 0 and −196 °C cold traps resulted in collection of the product in the −196 °C trap. Yield: 11.7 g (88% based on $H_2{}^{18}O$). The $^{19}F$ NMR spectrum of this compound was identical with that of the natural abundance compound.


(4) Seppelt, K. *Angew. Chem., Int. Ed. Engl.* **1982**, *21*, 877.
(5) Engelbrecht, A.; Sladky, F. *Adv. Inorg. Chem. Radiochem.* **1981**, *24*, 189.
(6) Seppelt, K. *Acc. Chem. Res.* **1979**, *12*, 211.
(7) Seppelt, K. *Z. Anorg. Allg. Chem.* **1973**, *399*, 65.
(8) Engelbrecht, A.; Sladky, F. *Int. Rev. Sci.: Inorg. Chem., Ser. Two* **1975**, *3*, 137.
(9) Seppelt, K. *Z. Anorg. Allg. Chem.* **1973**, *399*, 87.
(10) Mayer, E.; Sladky, F. *Inorg. Chem.* **1975**, *14*, 589.
(11) Sladky, F.; Kropshofer, H.; Leitzke, O.; Peringer, P. *J. Inorg. Nucl. Chem., Suppl.* **1976**, 69.
(12) Kemmit, R. D. W.; Russell, D. R.; Sharp, D. W. A. *J. Chem. Soc.* **1963**, 4408.
(13) Hepworth, M. A.; Jack, K. H.; Westland, G. *J. Inorg. Nucl. Chem.* **1956**, *2*, 79.
(14) Rappé, A. K. *J. Chem. Phys.* **1986**, *85*, 6576.
(15) Shriver, D. F.; Drezdzon, M. A. *The Manipulation of Air-Sensitive Compounds*, 2nd ed.; Wiley-Interscience: New York, 1986.
(16) Schack, C. J.; Wilson, W. W.; Christe, K. O. *Inorg. Chem.* **1983**, *22*, 18.
(17) Sladky, F. *Inorg. Synth.* **1986**, *24*, 34.

**Table II.** Atomic Coordinates ($\times 10^4$) and Isotropic Thermal Parameters ($Å^2 \times 10^3$)[a] for $[(PS)H^+][OTeF_5^-]$

| atom | x | y | z | $U_{iso}$[b] |
|---|---|---|---|---|
| Te | 2433 (1) | 3529 (1) | 3170 (1) | 24 (1) |
| O | 3264 (3) | 3003 (3) | 4442 (2) | 45 (1) |
| F1 | 1520 (3) | 4145 (2) | 1867 (2) | 45 (1) |
| F2 | 1706 (2) | 5629 (2) | 3235 (2) | 47 (1) |
| F3 | 4376 (2) | 4206 (2) | 2261 (2) | 53 (1) |
| F4 | 3012 (2) | 1544 (2) | 2867 (2) | 42 (1) |
| F5 | 300 (2) | 3002 (2) | 3846 (2) | 42 (1) |
| C1 | 3162 (3) | 1785 (3) | 8250 (2) | 24 (1) |
| C2 | 3577 (4) | 2534 (4) | 8959 (3) | 32 (1) |
| C3 | 3402 (4) | 1826 (4) | 10110 (3) | 38 (1) |
| C4 | 2824 (4) | 373 (4) | 10540 (3) | 36 (1) |
| C5 | 2386 (3) | -445 (4) | 9831 (2) | 30 (1) |
| C6 | 2512 (3) | 284 (3) | 8657 (2) | 24 (1) |
| C7 | 1825 (4) | -1966 (4) | 10261 (3) | 37 (1) |
| C8 | 1394 (4) | -2746 (4) | 9597 (3) | 41 (1) |
| C9 | 1443 (4) | -2019 (3) | 8431 (3) | 33 (1) |
| C10 | 1982 (3) | -551 (3) | 7982 (2) | 23 (1) |
| C11 | 2588 (4) | 4165 (3) | 6723 (3) | 31 (1) |
| C12 | 5203 (3) | 2381 (3) | 6529 (2) | 28 (1) |
| C13 | 247 (3) | 836 (3) | 6580 (2) | 27 (1) |
| C14 | 2891 (4) | -733 (3) | 6020 (3) | 32 (1) |
| N1 | 3408 (3) | 2496 (2) | 7032 (2) | 21 (1) |
| N2 | 1979 (3) | 243 (3) | 6800 (2) | 22 (1) |
| H | 2865 (58) | 1568 (47) | 6736 (35) | 84 (16) |

[a] Estimated standard deviations in the least significant digits are given in parentheses. [b] The equivalent isotropic $U$ is defined as one-third of the trace of the $U_{ij}$ tensor except for the hydrogen atom, which was refined isotropically.

**Table III.** Bond Distances (Å) and Angles (deg) for the $OTeF_5^-$ Anion in $[(PS)H^+][OTeF_5^-]$[a]

| | | | |
|---|---|---|---|
| Te-O | 1.786 (3) [1.803] | Te-F1 | 1.854 (2) [1.872] |
| Te-F2 | 1.856 (2) [1.871] | Te-F3 | 1.848 (2) [1.867] |
| Te-F4 | 1.846 (2) [1.862] | Te-F5 | 1.862 (2) [1.879] |

| | | | |
|---|---|---|---|
| O-Te-F1 | 177.7 (1) | O-Te-F2 | 94.4 (1) |
| F1-Te-F2 | 83.4 (1) | O-Te-F3 | 95.1 (1) |
| F1-Te-F3 | 85.6 (1) | F2-Te-F3 | 88.6 (1) |
| O-Te-F4 | 95.8 (1) | F1-Te-F4 | 86.4 (1) |
| F2-Te-F4 | 169.8 (1) | F3-Te-F4 | 90.2 (1) |
| O-Te-F5 | 95.5 (1) | F1-Te-F5 | 83.8 (1) |
| F2-Te-F5 | 89.1 (1) | F3-Te-F5 | 169.3 (1) |
| F4-Te-F5 | 90.2 (1) | | |

[a] Estimated standard deviations in the least significant digits are given in parentheses. Values in square brackets are librationally corrected distances (see text).

**Crystallographic Studies.** A colorless crystal of $[(PS)H^+][OTeF_5^-]$ was centered on a Nicolet R3m diffractometer. Centering of 25 reflections allowed least-squares calculation[18] of the cell constants given in Table I. Other experimental parameters are also listed in Table I.

The intensities of control reflections (400, 030, 006) monitored every 97 reflections showed no significant trend during the course of the data collection. An empirical absorption correction, based on intensity profiles for 16 reflections over a range of setting angles ($\psi$) for the diffraction vector, was applied to the observed data. The transmission factors ranged from 0.980 to 0.743. Lorentz and polarization corrections were applied to the data.

The structure was solved by direct methods (program SOLV).[18] The refinements involved anisotropic thermal parameters for all non-hydrogen atoms. The hydrogen atom bridging the two nitrogen atoms was located and refined isotropically. The other hydrogen atoms were included in calculated positions (C-H = 0.96 Å, $U(H) = 1.2U_{iso}(C)$). Neutral-atom scattering factors (including anomalous scattering) were taken from ref 19. The weighted least-squares refinements converged (weights calculated as $(\sigma^2(F) + |g|F_o^2)^{-1}$), with the average shift/esd < 0.010 over the last six cycles. In the final difference Fourier map, the maximum and minimum electron densities were 0.66 (near Te) and -0.51 e $Å^{-3}$. Analysis of variance as a function of Bragg angle, magnitude of $F_o$, reflection indices, etc. showed no significant trends.

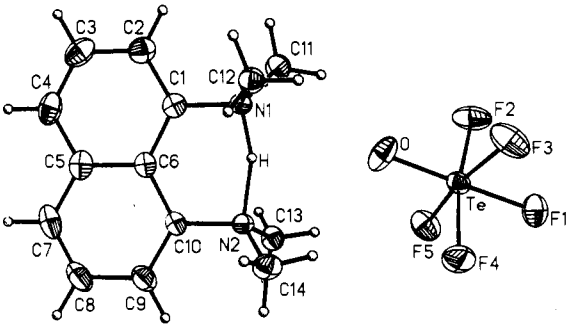


**Figure 1.** Drawing of the $OTeF_5^-$ anion and the protonated Proton Sponge cation ($(PS)H^+$) in $[(PS)H^+][OTeF_5^-]$ (50% probability ellipsoids). The separation of the ions is to scale.

Table II contains a list of atomic positional parameters and equivalent isotropic thermal parameters for all non-hydrogen atoms. Table III contains a list of bond distances and angles for the $OTeF_5^-$ anion. Available as supplementary material are a stereoview of the unit cell packing of $[(PS)H^+][OTeF_5^-]$ (Figure S-1) and lists of anisotropic thermal parameters for all non-hydrogen atoms (Table S-I), hydrogen atom positions and isotropic thermal parameters (Table S-II), bond distances and angles for the $(PS)H^+$ cation (Table S-III), and observed and calculated structure factors (Table S-IV). See paragraph at end of paper regarding supplementary material.

**Theoretical Details.** All Hartree-Fock (HF) calculations were performed with the Wadt and Hay relativistic ab inito tellurium effective core potential.[20] The tellurium valence s and p basis was also taken from Wadt and Hay.[20] The sets of tellurium d functions and the linear terms in the fluorine valence-double-$\zeta$ basis were those that had been optimized for $TeF_6$.[14] The oxygen basis consisted of the Dunning-Huzinaga valence-double-$\zeta$ basis augmented by a set of diffuse p functions, $\zeta = 0.059$, and a set of d functions, $\zeta = 0.85$.[21] The sodium effective core potential and basis of Melius and Goddard were used.[22] All reported geometries were obtained by using analytic HF gradient techniques and were restricted to $C_{2v}$ symmetry; except for the $OTeF_5$ radical, all of the structures refined to $C_{4v}$ symmetry. The $A_1$ vibrational stretching frequencies were obtained by finite differences of the analytic gradients. The reported frequencies have been scaled by 0.9, reflecting the observation that harmonic frequencies calculated at the HF level are consistently about 10-15% higher than the corresponding experimental frequencies.[23]

## Results

**Preparation of $H^{18}OTeF_5$.** The usual synthesis of $HOTeF_5$ (eq 1),[3,16,24] could not be employed to prepare its oxygen-18 equivalent.

$$Te(OH)_6 + 5HSO_3F \xrightarrow[\text{reflux}]{HSO_3F} HOTeF_5 + 5H_2SO_4 \quad (1)$$

Furthermore, the direct combination of $TeF_6$ and $H_2{}^{18}O$ is not synthetically useful.

The following reaction scheme (eq 2-4), based on an $^{18}OH^-/F^-$ metathesis, afforded a high yield of $H^{18}OTeF_5$ (88% based on $H_2{}^{18}O$, py = pyridine).

$$H_2{}^{18}O + CaH_2 \xrightarrow{py} 2H_2 + Ca(^{18}OH)_2 \quad (2)$$

$$Ca(^{18}OH)_2 + 2TeF_6 \xrightarrow[12h]{py,\ 45\ ^\circ C} CaF_2 + 2[pyH^+][^{18}OTeF_5^-] \quad (3)$$

$$[pyH^+][^{18}OTeF_5^-] + \text{excess } H_2SO_4 \rightarrow [pyH^+][HSO_4^-] + H^{18}OTeF_5 \quad (4)$$

(18) Calculations for diffractometer operations were performed by using software supplied with the Nicolet R3m diffractometer. All structural calculations were performed on the Data General Eclipse S/140 computer in the X-ray laboratory at Colorado State University with the SHELXTL program library written by Professor G. M. Sheldrick and supplied by Nicolet XRD Corp.

(19) *International Tables for X-ray Crystallography*; Kynoch: Birmingham, England, 1974; Vol. IV.

(20) Wadt, W. R.; Hay, P. J. *J. Chem. Phys.* **1985**, *82*, 284.

(21) Dunning, T. H.; Hay, P. J. *Modern Theoretical Chemistry: Methods of Electronic Structure Theory*; Schaefer, H. F., III, Ed.; Plenum: New York, 1977; Vol. 3, p 79.

(22) Melius, C. F.; Goddard, W. A., III. *Chem. Phys. Lett.* **1972**, *15*, 524.

(23) Pople, J. A.; Schlegel, H. B.; Krishnan, R.; DeFrees, D. J.; Binkley, J. S.; Frisch, M. J.; Whiteside, R. A. *Int. J. Quantum Chem., Quantum Chem. Symp.* **1981**, *15*, 269.

(24) Seppelt, K.; Nothe, D. *Inorg. Chem.* **1973**, *12*, 2727.

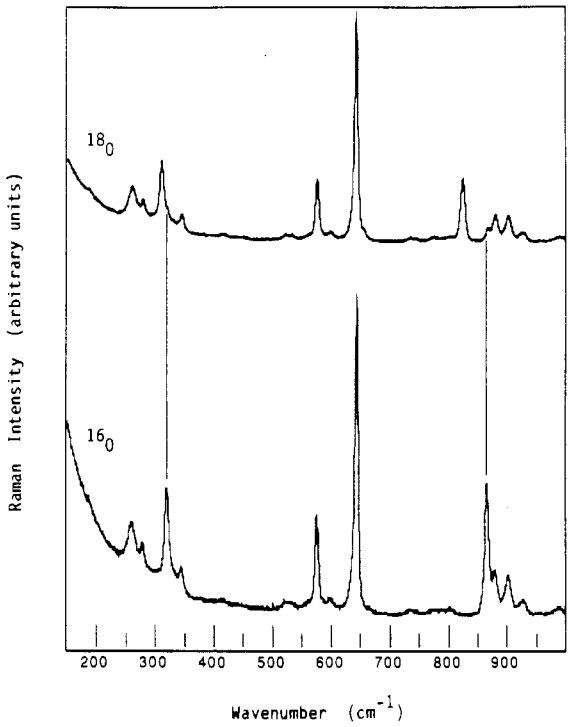


**Figure 2.** Raman spectra (514.5-nm excitation) of the $^{16}O$ (bottom) and $^{18}O$ (top) equivalents of $[N(n\text{-}Bu)_4^+][OTeF_5^-]$.

**Structure of $[(PS)H^+][OTeF_5^-]$.** Figure 1 shows drawings of the cation and anion, as well as the numbering scheme used. The separation of the ions is to scale. The bond distances and angles within the $(PS)H^+$ cation are normal (see Table S-III).[25]

The structural results (distances, angles, and thermal parameters) leave little doubt that the teflate anion in this salt has been oriented by the anisotropic cation and does not exhibit the O/F disorder observed for alkali-metal salts of $OTeF_5^-$.[11] For example, the equivalent isotropic thermal parameter ($U_{iso}$) of the oxygen atom is the same as those for the five fluorine atoms (Table II), a strong indication that the atom assigned as oxygen in this structure does indeed have eight electrons. Furthermore, the Te–O distance in this salt is significantly shorter than the Te–F distances (as expected), and the O–Te–$F_{eq}$ angles are all ~95° (Table III). Any significant amount of O/F disorder would be manifested as a smearing out of the electron density associated with the oxygen and fluorine atoms, resulting in anomalously large thermal parameters for these atoms along the Te–O or Te–F bonds. Note that $U_{iso}$ for the oxygen and fluorine atoms are smaller than those of the oxygen and fluorine atoms of structurally characterized teflate compounds for which X-ray data were collected at low temperatures.[3,26-28] The distance between the teflate oxygen atom and the N–H–N proton is 2.79 (4) Å.

As usual for $OTeF_5$ compounds, the oxygen and fluorine atoms in this structure exhibit relatively large amplitude thermal motion (see Tables II and S-I), despite the low temperature at which the data set was collected. A standard rigid-body librational analysis was performed,[29] resulting in $R = 0.038$. As expected, the librationally corrected Te–O and Te–F bond distances are longer than the uncorrected distances (see Table III). The librationally corrected O···H distance is 2.78 Å.

(25) (a) Truter, M. R.; Vickery, B. L. *J. Chem. Soc., Dalton Trans.* **1972**, 395. (b) Einspahr, H.; Robert, J.-B.; Marsh, R. E.; Roberts, J. D. *Acta Crystallogr., Sect B: Struct. Crystallogr. Cryst. Chem.* **1973**, *B29*, 1611.
(26) Strauss, S. H.; Noirot, M. D.; Anderson, O. P. *Inorg. Chem.* **1985**, *24*, 4307.
(27) Strauss, S. H.; Noirot, M. D.; Anderson, O. P. *Inorg. Chem.* **1986**, *25*, 3850.
(28) Noirot, M. D.; Anderson, O. P.; Strauss, S. H. *Inorg. Chem.* **1987**, *26*, 2216.
(29) Schomaker, V.; Trueblood, K. N. *Acta Crystallogr., Sect B: Struct. Crystallogr. Cryst. Chem.* **1968**, *B24*, 63.

**Table IV.** $\nu$(TeO) and $\nu$(TeF) Data ($cm^{-1}$) for $OTeF_5^-$ Salts[a]

| mode | $[N(n\text{-}Bu)_4^+][OTeF_5^-]$ | $[(PS)H^+][OTeF_5^-]$ |
|---|---|---|
| $\nu(Te^{16}O)$ IR, R | 867, 866 | 865, 867 |
| $\nu(Te^{18}O)$ IR, R | 825, 826 | 825, *b* |
| $\nu$(TeF) IR, $^{16}O$ | 635, 576 | 637, 578 |
| $\nu$(TeF) IR, $^{18}O$ | 635, 576 | 635, 578 |
| $\nu$(TeF) R, $^{16}O$ | 645, 576 | 651, 580 |
| $\nu$(TeF) R, $^{18}O$ | 644, 576 | *b* |

[a] Solid-state spectra at 22 °C. [b] A Raman spectrum of $[(PS)H^+][^{18}OTeF_5^-]$ was not recorded.

**Table V.** Vibrational Data ($cm^{-1}$) and Assignments for $OTeF_5^-$ Salts[a]

| | | | $[N(n\text{-}Bu)_4^+][OTeF_5^-]$[c] | | |
|---|---|---|---|---|---|
| sym | mode[b] | assignment | $^{16}O$ | $^{18}O$ | $Cs^+OTeF_5^-$[d] |
| $A_1$ | $\nu_1$ | $\nu$(TeO) | 867 | 825 | 873 |
| | $\nu_2$ | $\nu_{sym}(TeF_4)$ | 645 | 644 | 650 |
| | $\nu_3$ | $\nu(TeF_{ax})$ | 576 | 576 | 578 |
| | $\nu_4$ | $\delta_{sym}(TeF_4)$ out-of-plane bend | 345 | 345 | *e* |
| $B_1$ | $\nu_5$ | $\nu_{sym}(TeF_4)$ | *e* | *e* | *e* |
| | $\nu_6$ | $\delta_{asym}(TeF_4)$ out-of-plane bend | 260 | 261 | *e* |
| $B_2$ | $\nu_7$ | $\delta_{sym}(TeF_4)$ in-plane bend | *e* | *e* | *e* |
| E | $\nu_8$ | $\nu_{asym}(TeF_4)$ | 635 | 635 | 635 |
| | $\nu_9$ | $\delta(F_{ax}\text{–}Te\text{–}F_{eq})$ | 331 | 331 | 331 |
| | $\nu_{10}$ | $\delta(O\text{–}Te\text{–}F_{eq})$ | 320 | 310 | 315 |
| | $\nu_{11}$ | $\delta_{asym}(F_{eq}\text{–}Te\text{–}F_{eq})$ | 279 | 280 | 286 |

[a] Solid-state spectra at 22 °C. [b] The nomenclature used is consistent with that used for $IOF_5$ (see ref 32). [c] This work. [d] Reference 10. [e] Not observed.

**IR and Raman Data.** Spectra of $N(n\text{-}Bu)_4^+][OTeF_5^-]$, $[(PS)H^+][OTeF_5^-]$, and their oxygen-18 equivalents were recorded at 22 °C (a Raman spectrum of $[(PS)H^+][^{18}OTeF_5^-]$ was not recorded). The Raman spectra of $[N(n\text{-}Bu)_4^+][^{16}OTeF_5^-]$ and $[N(n\text{-}Bu)_4^+][^{18}OTeF_5^-]$ are shown in Figure 2. Bands assigned to TeO and TeF stretching normal modes are listed in Table IV. A complete list of the 11 fundamental vibrations for the $OTeF_5^-$ anion and observed frequencies for $[N(n\text{-}Bu)_4^+][^{16}OTeF_5^-]$ and $[N(n\text{-}Bu)_4^+][^{18}OTeF_5^-]$ are listed in Table V, which also includes data for $Cs^+OTeF_5^-$ from ref 10.

## Discussion

**Molecular Structure of $OTeF_5^-$.** One goal of this study was to establish the detailed molecular structure of the free teflate anion. This information would serve as a benchmark for structural comparisons with metal[26-28,30] and non-metal[3-6] teflates. Several papers have discussed the trend in Te–O distance as a function of the "degree of ionicity" of a M–$OTeF_5$ bond.[3-6,26-28,30]

Salts such as $Cs^+OTeF_5^-$ and $[N(n\text{-}Bu)_4^+][OTeF_5^-]$ are not suitable for structural studies because of the disorder they exhibit. Therefore, we sought a salt of $OTeF_5^-$ in which the cation would interact with the teflate oxygen atom just enough to orient it and overcome the oxygen/fluorine disorder, yet not enough to perturb the "free $OTeF_5^-$" character of the teflate group. The latter criterion would be established by the near congruence of IR and Raman spectral data for such a salt and $[N(n\text{-}Bu)_4^+][OTeF_5^-]$.

We believe that $[N(n\text{-}Bu)_4^+][OTeF_5^-]$ is a better model for free teflate than $Cs^+OTeF_5^-$, since the anion is better insulated from the positive charge. This is supported by the following observations. When a mixture of several equivalents of $HOTeF_5$ (bp 60 °C[31]) and solid $[N(n\text{-}Bu)_4^+][OTeF_5^-]$ are vacuum dried at 22 °C, the compound $[N(n\text{-}Bu)_4^+][H(OTeF_5)_2^-]$ is formed quantitatively.

(30) Strauss, S. H.; Abney, K. D.; Long, K. M.; Anderson, O. P. *Inorg. Chem.* **1984**, *23*, 1994.
(31) Engelbrecht, A.; Sladky, F. *Angew. Chem., Int. Ed. Engl.* **1964**, *3*, 383.

**Table VI.** Structural and Spectroscopic Data for $OTeF_5$ Compounds[a]

| compd | Te–O[b] | Te–F[c] | O–Te–$F_{eq}$[d] | $\nu$(TeO)[e] | $\delta_A$[f] |
|---|---|---|---|---|---|
| $[(PS)H^+][OTeF_5^-]$ | 1.803 | 1.870 | 95.2 | 865 | −20.0 |
| $Mn(CO)_5(OTeF_5)$[g] | 1.83 | 1.89 | 95.2 | 848 | −30.8 |
| $[N(n\text{-}Bu)_4^+][H(OTeF_5)_2^-]$[h] | 1.842 | 1.861 | 93.6 | 808[i] | −32.0 |
| $B(OTeF_5)_3$[j] | 1.883 | 1.837 | 92.6 | <740[k] | −46.2 |

[a] All data from this work unless otherwise noted. [b] Librationally corrected Te–O distance in Å. [c] Librationally corrected average Te–F distance in Å. [d] Average O–Te–$F_{eq}$ bond angle in deg. [e] Solid-state infrared Te–O stretching frequency in $cm^{-1}$. [f] $^{19}F$ NMR chemical shift ($CH_2Cl_2$, 22 °C, $CFCl_3$ internal standard) of fluorine trans to oxygen. [g] Reference 30. [h] Reference 3. [i] Average of two observed bands at 850 and 766 $cm^{-1}$. [j] Birchall, T.; Myers, R. D.; DeWaard, H.; Schrobilgen, G. J. *Inorg. Chem.* **1982**, *21*, 1068. [k] Highest energy band attributable to $\nu$(TeO) or $\nu$(TeF): Kropshofer, H.; Leitzke, O.; Peringer, P.; Sladky, F. *Z. Anorg. Allg. Chem.* **1973**, *399*, 65.

This salt is unchanged even after prolonged vacuum drying at 40 °C.[3] In contrast, a tensimetric titration of $Cs^+OTeF_5^-$ with $HOTeF_5$ shows only incomplete, reversible formation of $[Cs^+][H(OTeF_5)_2^-]$; the salt $Cs^+OTeF_5^-$ is recovered unchanged when a mixture of $HOTeF_5$ and $Cs^+OTeF_5^-$ is dried under vacuum at 22 °C. These experiments show that the lattice energy of $Cs^+OTeF_5^-$ and the concomitant perturbation of the anion must be substantially larger than those of $[N(n\text{-}Bu)_4^+][OTeF_5^-]$.

We prepared a series of salts in which $OTeF_5^-$ is progressively more weakly hydrogen bonded to a variety of $BH^+$ cations (B = a nitrogenous Brønsted base). These include the following (cation, $\nu$(TeO) in $cm^{-1}$): $pyH^+$ (py = pyridine), 843 and 852; $lutH^+$ (lut = lutidine), 845; $NEt_3H^+$, 852;[3] $(PS)H^+$, 865.

The salt $[(PS)H^+][OTeF_5^-]$ has the closest match of $\nu$(TeO) with $[N(n\text{-}Bu)_4^+][OTeF_5^-]$, and thus serves as the best ordered model for free teflate available. Comparisons can be made with the other teflate compounds for which librationally corrected bond distances are available, $Mn(CO)_5(OTeF_5)$, $[N(n\text{-}Bu)_4^+][H(OTeF_5)_2^-]$, and $B(OTeF_5)_3$ (Table VI). The structure of free, ionic $OTeF_5^-$ has the shortest Te–O bond, 1.803 Å, of all of these compounds. The free teflate data in Table VI are consistent with the established trends:[3-8] in general, as the negative charge of a teflate group is more and more localized on the oxygen atom, the Te–O bond shortens, the Te–F bonds lengthen, the O–Te–$F_{eq}$ angles increase, the Te–O stretching frequency increases, and the $^{19}F$ NMR chemical shift of the fluorine atom trans to oxygen shifts upfield.

**Electronic Structure of $OTeF_5^-$.** Our structural data for free teflate, along with vibrational data for the oxygen-18 equivalent of $[N(n\text{-}Bu)_4^+][OTeF_5^-]$, have allowed us to improve the vibrational analysis of $OTeF_5^-$ published by Mayer and Sladky in 1975.[10] They assumed, for a $C_{4v}$ $OTeF_5^-$ anion, Te–O = 1.70 Å, Te–$F_{ax}$ = Te–$F_{eq}$ = 1.84 Å, and all angles = 90°.

In addition to Mayer and Sladky's study of $Cs^+OTeF_5^-$,[10] vibrational data are available for the following $C_{4v}$ or pseudo-$C_{4v}$ $XYF_5$ molecules or ions with octahedral central atoms: $IOF_5$,[32] $HOTeF_5$,[33] $ClTeF_5$,[34] $XOTeF_5$ (X = F, Cl),[35] $HOSeF_5$,[36] $ClSeF_5$,[37] $XOSeF_5$ (X = F, Cl, Br),[36] $OSeF_5^-$,[10,36] $ClSF_5$,[38] and $OSF_5^-$.[39] Another relevant species for which data have been reported is the $OXeF_5^-$ anion,[40] although the central xenon atom is almost certainly distorted from $C_{4v}$ symmetry by its lone pair of electrons.

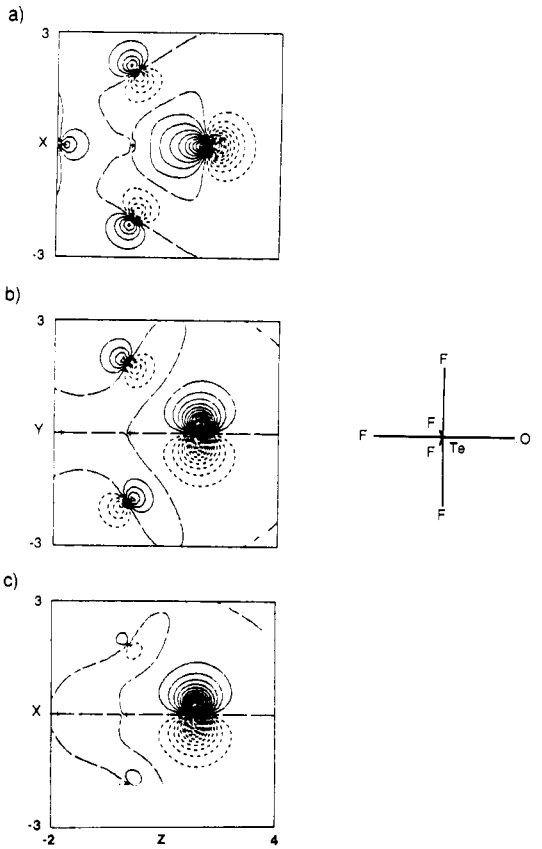


**Figure 3.** Contour plots of the canonical Hartree–Fock orbitals defining the three oxygen valence p orbitals (the HOMO's of $a_1$, $b_1$, and $b_2$ symmetry) for the $OTeF_5$ radical. The solid contours define positive amplitude (spaced at 0.05 au), the dashed contours define negative amplitude, and the long dashed lines define nodal lines. The plotting planes contain O, Te, $F_{ax}$, and two $F_{eq}$ atoms: (a) the Te–O $\sigma$ bond; (b) the O lone pair; (c) the O radical p orbital.

The assignment of the 11 fundamentals for $OTeF_5^-$ is shown in Table V, along with nine observed frequencies for the $^{16}O$ and $^{18}O$ equivalents of $[N(n\text{-}Bu)_4^+][OTeF_5^-]$ and seven observed frequencies (taken from ref 10) for solid-state spectra of $Cs^+OTeF_5^-$. The assignment follows the one detailed in ref 10. The $A_1$ and E modes are IR and Raman active, while the B modes should be Raman active only.

A normal-coordinate analysis was carried out for the $OTeF_5^-$ anion by using IR and Raman data for the $^{16}O$ and $^{18}O$ equivalents of $[N(n\text{-}Bu)_4^+][OTeF_5^-]$ and structural data for $[(PS)H^+][OTeF_5^-]$. $C_{4v}$ symmetry was assumed. The calculations were carried out by using the QCMP012 conversion of the QCPE 342 programs.[41] These programs refine a set of force constants to give a least-squares fit to the observed frequencies by using the Wilson *FG* method. The methodology used and all of the results of these calculations are given in the supplementary material. With one exception, our refined set of 16 force constants allowed the frequencies of the $^{16}O$ and $^{18}O$ equivalents of $[N(n\text{-}Bu)_4^+][OTeF_5^-]$ to be matched to within 1 $cm^{-1}$, the accuracy of the reported frequencies: $\nu_{11}$ for $[N(n\text{-}Bu)_4^+][^{18}OTeF_5^-]$ was found to be 280 $cm^{-1}$ and predicted to be 277 $cm^{-1}$. The frequencies for $\nu_5$ and $\nu_7$ are predicted to be 658 and 347 $cm^{-1}$ for $^{16}OTeF_5^-$ and 658 and 346 $cm^{-1}$ for $^{18}OTeF_5^-$. Thus, $\nu_7$ may be masked by $\nu_4$, which is found at 345 $cm^{-1}$ in both isotopomers of $[N(n\text{-}Bu)_4^+][OTeF_5^-]$ (see Table V).

Our refined force constants are in excellent agreement with the 11 values from the supplementary material for ref 10 (eight

(32) Smith, D. F.; Begun, G. M. *J. Chem. Phys.* **1965**, *43*, 2001.
(33) Burger, H. *Z. Anorg. Allg. Chem.* **1968**, *360*, 97.
(34) Brooks, W. V. F.; Eshaque, M.; Lau, C.; Passmore, J. *Can. J. Chem.* **1976**, *54*, 817.
(35) Schack, C. J.; Wilson, W. W.; Christe, K. O. *Inorg. Chem.* **1983**, *22*, 18.
(36) Seppelt, K. *Z. Anorg. Allg. Chem.* **1973**, *399*, 87.
(37) Christe, K. O.; Schack, C. J.; Curtis, E. C. *Inorg. Chem.* **1972**, *11*, 583.
(38) Griffiths, J. E. *Spectrochim. Acta, Part A* **1967**, *23A*, 2145.
(39) Christe, K. O.; Schack, C. J.; Pilipovich, D.; Curtis, E. C.; Sawodny, W. *Inorg. Chem.* **1973**, *12*, 620.
(40) Holloway, J. H.; Kaucic, V.; Martin-Rovet, D.; Russell, D. R.; Schrobilgen, G. J.; Selig, H. *Inorg. Chem.* **1985**, *24*, 678.

(41) QCPE 342 is a set of "Generalized Vibrational Analysis Programs Utilizing the Wilson GF Matrix Method for a General Unsymmetrized Molecule", by D. F. McIntosh and M. R. Peterson. QCMP012 is a direct conversion of these programs for IBM personal computers and compatibles by T. J. O'Leary.

**Table VII.** Stretching Force Constants (mdyn/Å) for $OTeF_5^-$

| | | lit.[10] | this work |
|---|---|---|---|
| $f_S$ (lit. $f_O$) | Te–O str | 6.16 | 6.23 |
| $f_R$ | Te–$F_{ax}$ str | 3.38 | 3.23 |
| $f_r$ | Te–$F_{eq}$ str | 4.16 | 4.05 |
| $f_{rr}$ | interacn between adj Te–$F_{eq}$ str | −0.05 | −0.0562 |
| $f_{rr'}$ | interacn between opp Te–$F_{eq}$ str | 0.66 | 0.687 |
| $f_{RS}$ | interacn between Te–O and Te–$F_{ax}$ str | 0.18 ± 0.18 | 0.193 |

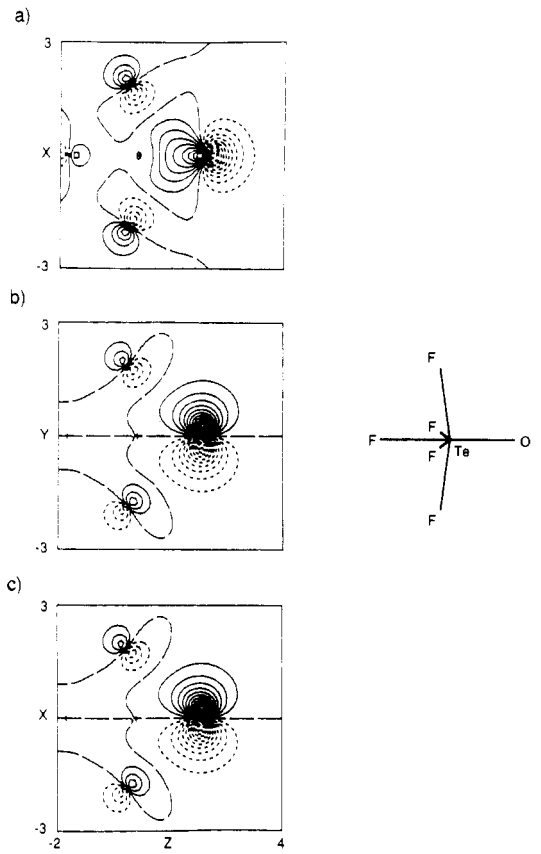


**Figure 4.** Contour plots of the canonical Hartree–Fock orbitals defining the three oxygen valence p orbitals (the HOMO's of $a_1$, $b_1$, and $b_2$ symmetry) for the $OTeF_5^-$ anion. The solid contours define positive amplitude (spaced at 0.05 au), the dashed contours define negative amplitude, and the long dashed lines define nodal lines. The plotting planes contain O, Te, $F_{ax}$, and two $F_{eq}$ atoms: (a) the Te–O $\sigma$ bond; (b) an O lone pair; (c) an O lone pair.

refined, three fixed at their $IOF_5$ values). For comparison, the six stretching force constants from our analysis and from ref 10 are shown in Table VII. The differences between the geometry assumed by Mayer and Sladky and the actual geometry of $OTeF_5^-$ are minor as far as the force field of the anion is concerned. Furthermore, the low value of $f_{RS}$ supports their tentative conclusion that it is proper to talk of individual Te–O and Te–$F_{ax}$ stretching frequencies.

We have carried out ab initio Hartree-Fock (HF) calculations on the $OTeF_5$ radical, $Na^+OTeF_5^-$, and the singlet and triplet states of $OTeF_5^-$. The refined geometries, net Mullikan charges, and frequencies for TeO and TeF stretching vibrations of $A_1$ symmetry are listed in Table VIII. The oxygen molecular orbitals are shown in Figures 3–5.

The calculated geometries for $Na^+OTeF_5^-$ and the ground (singlet) state of the free $OTeF_5^-$ anion are in agreement with the structure of $[(PS)H^+][OTeF_5^-]$. The O–Te–$F_{eq}$ bond angles are calculated to be a few degrees greater than 90°, in harmony with the average O–Te–$F_{eq}$ angle of 95.2° in the observed structure. The angle for the free anion is 2.8° larger than the observed angle, while that for the sodium ion pair is 0.2° smaller.

**Table VIII.** Theoretical Results: Distances (Å), Angles (deg), $A_1$ Stretching Frequencies ($cm^{-1}$), and Mullikan Populations

| | $OTeF_5^-$ | $Na^+OTeF_5^-$ | $^3OTeF_5^-$ | $OTeF_5$ |
|---|---|---|---|---|
| Te–O | 1.750 | 1.748 | 2.030 | 1.888 |
| Te–$F_{ax}$ | 1.883 | 1.867 | 1.962 | 1.842 |
| Te–$F_{eq}$ | 1.890 | 1.864 | 1.962, 1.963 | 1.847, 1.849 |
| Na–O | | 1.971 | | |
| O–Te–$F_{eq}$ | 97.97 | 95.04 | 91.37, 86.26 | 92.43, 89.07 |
| $\nu$(TeO) | 886[a] | 967 | | |
| $\nu$(TeF) | 615, 540[b] | 703, 609 | | |
| population | | | | |
| Te | 2.590 | 2.643 | 2.171 | 2.661 |
| O | −0.918 | −1.120 | −0.462 | −0.355 |
| $F_{ax}$ | −0.525 | −0.483 | −0.537 | −0.456 |
| $F_{eq}$ | −0.537 | −0.496 | −0.544, −0.542 | −0.463, −0.462 |
| Na | | 0.943 | | |

[a] The calculated $\nu$(TeO) value for $^{18}OTeF_5^-$ is 846 $cm^{-1}$. [b] The calculated $A_1$ $\nu$(TeF) values for $^{18}OTeF_5^-$ are 610 and 539 $cm^{-1}$.

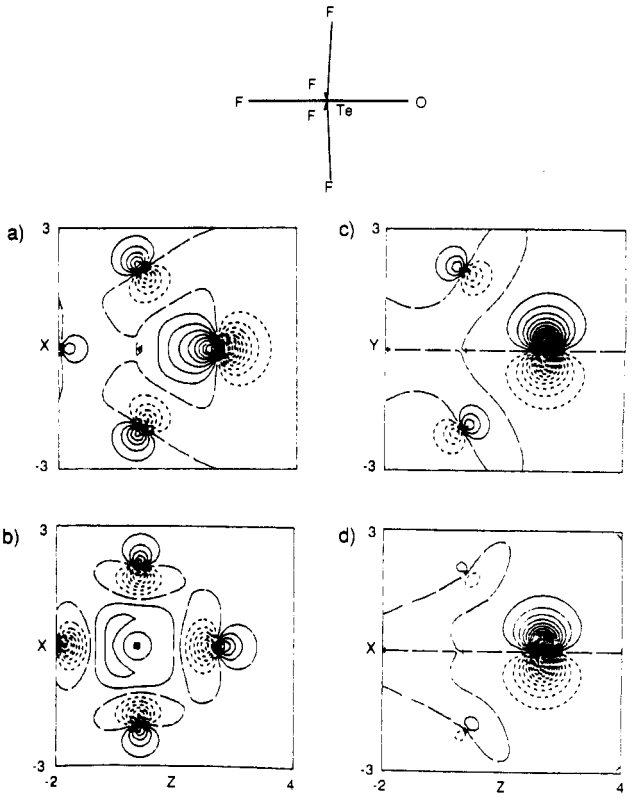


**Figure 5.** Contour plots of the canonical Hartree–Fock orbitals defining the three oxygen valence p orbitals (the HOMO's of $a_1$, $b_1$, and $b_2$ symmetry) for the $^3OTeF_5^-$ (triplet) anion. The solid contours define positive amplitude (spaced at 0.05 au), the dashed contours define negative amplitude, and the long dashed lines define nodal lines. The plotting planes contain O, Te, $F_{ax}$, and two $F_{eq}$ atoms: (a) the Te-O $\sigma$ bond; (b) the $a_1$ radical orbital; (c) the O p lone pair; (d) the O p radical orbital.

The calculated Te–F bond distance for the free anion is 0.02 Å longer than the average observed distance of 1.870 Å, while the distance for $Na^+OTeF_5^-$ matches the observed distance. In contrast, the calculated Te–O distances are both ~0.05 Å shorter than the observed distance of 1.803 Å. However, as we will argue below, the bonding between the tellurium and oxygen atoms in $OTeF_5^-$ has a large ionic component and should be very sensitive to the nature and position of the counterion. The calculations for the free anion were carried out in free space with no counterion present; those for $Na^+OTeF_5^-$ refined to a Na···O distance of 1.97 Å. If the sodium atom is fixed at a distance of 2.05 Å from the oxygen atom of the teflate anion, the calculated Te–O bond lengthens to 1.78 Å.

Calculated $\nu$(TeO) values for $OTeF_5^-$ and $Na^+OTeF_5^-$ are 19 and 100 $cm^{-1}$ higher, respectively, than the experimental value of 867 $cm^{-1}$, while calculated $\nu$(TeF) values are 30 and 36 $cm^{-1}$ too low for $OTeF_5^-$ and 58 and 33 $cm^{-1}$ too high for $Na^+OTeF_5^-$ when compared with the observed values of 645 and 576 $cm^{-1}$. The $\nu$(TeF) bands in Raman spectra of $[N(n\text{-}Bu)_4^+][OTeF_5^-]$ shift by 1 $cm^{-1}$ and <1 $cm^{-1}$ upon $^{18}O$ substitution (see Table IV). Our calculations have overestimated this vibrational coupling: we calculate shifts of 5 and 1 $cm^{-1}$ for $OTeF_5^-$ and 3 and 1 $cm^{-1}$ for $Na^+OTeF_5^-$.

The calculated geometry of the $OTeF_5$ radical is substantially different from that calculated for the teflate anion. The equatorial fluorine atoms that are coplanar with the singly occupied oxygen p orbital distort toward that radical orbital while the other two equatorial fluorine atoms distort away from the doubly occupied oxygen p orbital with which they are coplanar, leaving the $OTeF_5$ radical with only $C_{2v}$ symmetry. On going from the $OTeF_5^-$ anion to the $OTeF_5$ radical, the Te–F distances should shorten by 0.04 Å and the Te–O distance should lengthen by 0.14 Å. For a HF wave function, the calculated electron affinity of the $OTeF_5$ radical is 4.65 eV (cf. $TeF_6$, 3.10 eV[14]). A vibrational progression of 819 $cm^{-1}$ in the photodetachment spectrum of $OTeF_5^-$ is anticipated due to the substantial difference in TeO distances. The $OTeF_5$ radical has been generated by the photolysis of $Xe(OTeF_5)_2$ and identified by a matrix-isolation EPR experiment,[24] but little else is known about this species.

The molecular orbitals presented in Figures 3–5 demonstrate only a very slight change in Te–O $\pi$ bonding on going from the $OTeF_5$ radical to the free $OTeF_5^-$ anion (cf. Figure 3b,c with Figure 4b,c). Nevertheless, the Te–O bond strength of the anion is significantly greater than that of the radical, as shown by the shortening of the Te–O distance by 0.14 Å and an increase in $\nu$(TeO) by 67 $cm^{-1}$ on going from the radical to the anion. The difference in net Mullikan charges for these two species (Table VIII) shows that the increased Te–O bond strength of the free anion is due almost entirely to an increased electrostatic interaction between the positively charged tellurium atom and the negatively charged oxygen atom.

We have also calculated the geometry for the triplet excited state of $OTeF_5^-$, which is analogous to the bound state of $TeF_6^-$ (see Figure 5b).[14] This state is achieved by adding an electron to a symmetric tellurium orbital of the $OTeF_5$ radical rather than to the singly occupied p orbital on the oxygen atom (which would produce the singlet state of $OTeF_5^-$). The ground-state-singlet to excited-state-triplet excitation energy, calculated with a restricted HF wave function, is estimated to be ~15 000 $cm^{-1}$. The excited state has longer Te–O and Te–F bond distances, by 0.14 and 0.11 Å, respectively, relative to the ground state (cf. $TeF_6$ and $TeF_6^-$, where the distances differ by 0.11 Å[14]).

**Acknowledgment.** This research was supported by a grant from the NSF (CHE-8419719). We thank Professors J. R. Norton and A. T. Tu for the use of their IR and Raman spectrometers, respectively, Dr. B. I. Swanson for helpful discussions, and S. A. Ekberg, M. R. Colsman, L. F. Taylor, J. H. Reibenspies, and M. M. Miller for experimental assistance. P.K.M. thanks the Mobay Corp. for a Graduate Student Research Award. K.D.A. acknowledges the support of the Department of Energy. The Nicolet R3m/E diffractometer and computing system were purchased with NSF Grant No. CHE-8103011. Acknowledgment is made to the CSU Supercomputing Project for partial support of this research.

**Registry No.** $[pyH^+][OTeF_5^-]$, 40904-35-6; $[lutH^+][OTeF_5^-]$, 114595-21-0; $HOTeF_5$, 57458-27-2; $[(PS)H^+][OTeF_5^-]$, 114595-22-1; $H^{18}OTeF_5$, 114595-23-2; $CaH_2$, 7789-78-8; $TeF_6$, 7783-80-4; $OTeF_5^-$, 42503-56-0; $Na^+OTeF_5^-$, 53150-40-6; $OTeF_5$, 114595-24-3; $[N(n\text{-}Bu)_4^+][OTeF_5^-]$, 102648-79-3; $^{18}O$, 14797-71-8.

**Supplementary Material Available:** Figure S1, showing a stereoview of the packing of $[(PS)H^+][OTeF_5^-]$, Tables S-I, S-II, and S-III, respectively, listing thermal parameters, derived hydrogen positions, and bond distances and angles for the $(PS)H^+$ cation, and details of the vibrational analysis of the $OTeF_5^-$ anion (12 pages); Table S-IV, listing observed and calculated structure factors (19 pages). Ordering information is given on any current masthead page.

---

Contribution from the Solid State and Structural Chemistry Unit, Indian Institute of Science, Bangalore-560012, India

# Magnetic Susceptibility Studies on Ternary Oxides of Copper(II)†

K. Sreedhar and P. Ganguly*

*Received November 12, 1987*

The magnetic susceptibilities of a large number of ternary oxides of copper having structural features common to the presently identified phases of high-temperature superconductors have been studied in the temperature range 14–300 K. The systems studied are $Ln_2CuO_4$ (Ln = La, Pr, Nd, etc.), $Sr_2CuO_2Cl_2$, $Bi_2CuO_4$, $Ca_2CuO_3$, $Sr_2CuO_3$, $SrCuO_2$, $MgCu_2O_3$, $Ba_2Cu_3O_4Cl_2$, $Y_2Cu_2O_5$, $Y_2BaCuO_5$, $BaCuO_2$, $Li_2CuO_2$, etc. $Cu^{2+}$ ions take different coordinations, like isolated square planar, square pyramidal or distorted-tetrahedral and octahedral, in these compounds. These compounds also exhibit different varieties of possible magnetic superexchange interactions like 180° or 90° Cu–O–Cu or Cu–O–O–Cu types as well as direct Cu–Cu interactions. Compounds in which there are extended 180° Cu–O–Cu interactions show a low, nearly temperature-independent susceptibility ($100 \times 10^{-6}$ emu/mol). The estimated value of $J$ for the Cu–O–Cu interaction is between 800 and 1500 K in these compounds. Isolated $Cu^{2+}$ ions in which there are no 180° or close to 180° Cu–O–Cu interactions show Curie–Weiss susceptibility behavior. Compounds with only Cu–O–O–Cu interaction show evidence for the onset of antiferromagnetic coupling between 30 and 50 K. The superexchange rules are useful for explaining the qualitative features of the results. The possibility of disproportionation of $Cu^{2+}$ ion when there are short Cu–Cu distances as in $Bi_2CuO_4$ is discussed. The extended geometry of the copper–oxygen framework seems to be more important than the local geometry around the $Cu^{2+}$ ion in determining the magnetic properties.

## Introduction

The experimental developments, since the discovery of high-temperature superconductivity[1-3] in ternary oxide systems of copper with a low-dimensional component, have far outpaced the theoretical understanding.[4,5] Part of the reason for the theoretical

* To whom correspondence should be addressed.

† Contribution No. 487 from the Solid State and Structural Chemistry Unit.

(1) Bednorz, J. G.; Muller, K. A. *Z. Phys. B: Condens. Matter* **1986**, *64*, 189.

(2) Wu, M. K.; Ashburn, J. R.; Torng, C. J.; Hor, P. H.; Meng, R. L.; Gao, L.; Huang, J.; Wang, Y. Q.; Chu, C. W. *Phys. Rev. Lett.* **1987**, *58*, 908.

0020-1669/88/1327-2261$01.50/0 